Effects of entropy inhomogeneity on density-temperature correlation in solar wind

Francesco Malara, Leonardo Primavera, and Pierluigi Veltri
Dipartimento di Fisica, Università della Calabria, 87030 Arcavacata di Rende (CS), Italy
and Istituto Nazionale Fisica della Materia, Unità di Cosenza, 87030 Arcavacata di Rende (CS), Italy
(Received 30 July 1998)

Compressive fluctuations in solar wind slow speed streams are studied by means of a magnetohydrodynamics (MHD) model, which represents the plasma in the vicinity of the heliospheric current sheet. The model contains a current sheet, as well as density and temperature variations, corresponding to a large scale modulation of the specific entropy. Alfvénic fluctuations are initially superimposed on the background equilibrium and compressive fluctuations are consequently generated during the time evolution. The resulting correlation between density and temperature fluctuations at various spatial scales is interpreted in terms of both generation of magnetosonic fluctuations and of an ''entropy cascade.'' The latter phenomenon arises as a consequence of the interaction between the MHD turbulence and the underlying large scale entropy structure. In particular, it is responsible for anticorrelated density and temperature fluctuations detected at various scales. The results of the model are compared with the proton density-temperature correlation calculated during several crossings of solar wind slow speed streams by the Helios spacecraft. The model reproduces to a good extent the main observed features, in particular the dependence of the correlation coefficient on location (close to or far from the current sheet) and on the fluctuation scale. The results show that large scale inhomogeneities, in particular, that of specific entropy, are important ingredients in the dynamics of the MHD turbulence in slow speed streams. [S1063-651X(99)03505-9]

PACS number(s): 52.30.−q, 52.65.Kj, 96.60.Vg, 96.50.Bh

I. INTRODUCTION AND MOTIVATIONS

In the solar wind low-frequency range ($1\ \text{min} < t < 1$ day), compressive fluctuations are mainly observed in slow speed streams, close to the heliospheric current sheet, a much lower level of compressive fluctuations being observed in fast streams. Space data analyses have been performed to characterize these compressive fluctuations, mainly through the study of the correlation between fluctuations either of proton density (δn) and magnetic field intensity (δB) or of proton density (δn) and temperature (δT_p).

As concerns the former correlation Vellante and Lazarus [1] have shown that for fluctuations at time scales larger (smaller) than $t_c \sim 10$ h, positive (negative) correlations prevail. More detailed analyses [2], which have been carried out in selected slow speed streams in the inner heliosphere, have shown that in some cases the correlation remains negative also at large scales.

This phenomenology has been studied by us in two previous papers (Refs. [3] and [4] hereinafter referred to as paper I). In these papers we supposed that properties of compressible fluctuations were strictly related to the inhomogeneous character of the turbulence in slow speed streams, due to the presence of the large scale current sheet. To take into account this inhomogeneity, we have built up [3] a compressible numerical magnetohydrodynamics (MHD) model of the plasma around the heliospheric current sheet. We have then studied the propagation of Alfvénic fluctuations, which, starting from solar corona, converge on the two sides of the heliospheric current sheet. The dynamical evolution of such fluctuations displays a drastic change of their characteristics and in particular, it can be shown that compressible fluctuations are generated. In paper I we have analyzed the properties of these compressible fluctuations and compared them with those derived from space data obtaining a fine agreement, in particular as concerns the occurrence of both signs of observed δn-δB correlation and how this occurrence is related to (i) fluctuations spatial scale, (ii) location with respect to the current sheet, (iii) value of the plasma β.

The correlation between proton density and temperature on solar wind fluctuations has been studied by a number of authors [5–8]. In particular, Bavassano *et al.* [8] studied the properties of the compressive turbulence for the solar wind in the inner heliosphere by using Helios data. These authors carried out a detailed analysis of the density-temperature correlation as a function of the solar wind speed and the radial distance from the Sun, always in the inner heliosphere. They found that in general, cases with a well defined sign of the density-temperature correlation are seldom observed in solar wind, with very few cases reaching a value greater than 0.8 (as absolute value) for the correlation coefficient. Moreover, they found that on smaller scales, the sign of the correlation is mainly positive in fast streams, while both signs are present in slow streams.

From a theoretical point of view, correlation between density ρ and temperature T in MHD turbulence has been considered within the so-called Nearly incompressible magnetohydrodynamics (NI-MHD) theory [9–13], in which the limit of small sonic Mach number M is studied, i.e., small departures from incompressibility are considered. If the fluid is considered as a polytrope [heat-fluctuations-modified fluid (HFMF)], this theory predicts positive ρ-T correlations, as well as density fluctuations, scaling as the squared sonic Mach number [$\delta\rho/\rho \propto O(M^2)$]. On the contrary, if heat conduction is allowed [for heat-fluctuations-dominated fluid (HFDF)], the density-temperature correlation is expected as negative, and $\delta\rho/\rho \propto O(M)$. Klein *et al.* [5] have analyzed such scalings in solar wind data. They found that slow speed

streams fit well the predictions of NI-MHD theory for a HFDF, while the situation is rather ambiguous in fast streams. More recently, Bavassano *et al.* [8] considered the scalings of the density fluctuations with the sonic Mach number for the cases where the sign of the correlation was better defined, without finding the expected trend foreseen by the NI-MHD theory. These results have to be related to the ones of Matthaeus *et al.* [11] who performed an analogous analysis for the aforementioned scalings in the outer heliosphere without finding a clear evidence of them in the data.

From the above results, we have been pushed to look for an alternative solution to the problem posed by presence of negative n-T_p correlation in slow speed streams. This solution is based on an idea similar to the one used in our previous model [4,3], namely, the main ingredient is the inhomogeneity of the background medium. On the contrary, turbulence models which describes a statistically homogeneous situation (such as the NI-MHD theory) neglect such an ingredient, and assume that the background is spatially homogeneous.

In order to illustrate the physical mechanism which we propose, let us consider the evolution equation of the entropy per-mass-unit s, within the MHD framework [14]

$$\rho T\left(\frac{\partial}{\partial t}+\mathbf{v}\cdot\boldsymbol{\nabla}\right)s=Q+\boldsymbol{\nabla}\cdot\mathbf{q}. \tag{1}$$

In this equation Q represents heat sources, $\mathbf{q}$ is the heat flux, while $\mathbf{v}$, ρ, and T are the velocity, density, and temperature, respectively. The right-hand side contains the time derivative of s along the flow lines. In an ideal case, when energy dissipation and heat conduction are both neglected ($Q=0$, $\mathbf{q}=0$), the entropy s is simply convected by the fluid motion. So, if s is spatially homogeneous at the initial time, it will remain uniform during all the time. Such a configuration is referred to as *isoentropic*. In an isoentropic situation, compressive perturbations necessarily have density and temperature *positively correlated*. In fact since, in a perfect gas,

$$s\propto\ln\left(\frac{T}{\rho^{\gamma-1}}\right) \tag{2}$$

(γ being the adiabatic index), $s=$uniform during all the time implies

$$T\propto\rho^{\gamma-1}, \tag{3}$$

i.e., positive (negative) variations of ρ correspond to positive (negative) variations of T. For instance, this situation is typically recovered when (as usual in many MHD turbulence models) the polytropic equation $p/\rho^{\gamma}=$const is assumed, which is equivalent to the condition (3).

Concerning this point, we note also that when the above polytropic equation is assumed, only magnetosonic waves are found as small amplitude compressive perturbations. In such waves density and temperature are always positively correlated. In a more general case, when the polytropic equation is relaxed, also entropy waves can be found among the small amplitude compressive perturbations [14]. In entropy waves density and temperature fluctuations are anticorrelated, and the isoentropic condition ($s=$uniform) is clearly violated.

From the above discussion it is clear that density-temperature negative correlations require a nonuniform entropy distribution. In the statistically homogeneous situation considered by the NI-MHD heat-fluctuations-dominated fluid model [10], this is achieved by including the effects of the heat conduction. Heat conduction represents a source for entropy modulation [see Eq. (1)], and it can generate density-temperature negative correlations also in an initially isoentropic configuration. On the contrary, in the model which we propose the entropy modulation is not due to nonideal effects such as heat conduction, but it is assumed to be present from the outset, in the large scale inhomogeneity of the background structure.

Slow speed streams are colder and denser than the surrounding fast speed streams. So, when moving from a slow to a fast stream, the density and the temperature variations at large scale are anticorrelated. In other words, the entropy per-mass-unit s changes, being smaller in a slow stream than in the surrounding fast streams. This large scale variation of s has been explicitly taken into account in the present model, by including it in the background structure. It represents the new ingredient of the present model, which was lacking in the previous one (paper I).

Similar to our previous model, Alfvénic perturbations are initially superposed on the background, and a spectrum of velocity fluctuations forms. As a result, the coupling between the large scale entropy inhomogeneity and the Alfvénic perturbation [represented by the second term in the left-hand side of Eq. (1)], will move the entropy modulation to increasingly smaller scales. This mechanism is then able to produce density-temperature negative correlations at all the scales. On the other hand, as we have shown in paper I, the coupling between the Alfvénic perturbation and the large scale current sheet produces also magnetosoniclike fluctuations, in which density and temperature are positively correlated. As a result, the actual sign of the ρ-T correlation, at differents scales and locations, will be determined by the competition between these two mechanisms (entropy cascade and production of magnetosoniclike fluctuations).

The paper is organized as follows. In the next section both the physical and the numerical models are shortly reviewed. Then the main results of the simulation are described in Sec. III and further discussed in the last section.

II. THE MODEL

The numerical model derives from that used in previous papers [3,4], the main difference being in the initial condition. Here we report its main characteristics, referring the reader to the above-cited papers for a more detailed description. We integrated the nonlinear, dimensionless, magnetohydrodynamics (MHD) equations in $2+1/2$ dimensions for a compressible plasma. Viscosity, resistivity and thermal conduction terms are included in the equations of momentum, induction, and energy balance:

$$\frac{\partial\rho}{\partial\tau}+\boldsymbol{\nabla}\cdot(\rho\mathbf{v})=0, \tag{4}$$

$$\frac{\partial \mathbf{v}}{\partial \tau}+(\mathbf{v}\cdot\boldsymbol{\nabla})\mathbf{v}=-\frac{1}{\rho}\boldsymbol{\nabla}(\rho T)+\frac{1}{\rho}\mathbf{j}\times\mathbf{b}+\frac{1}{\rho S_\nu}\boldsymbol{\nabla}^2\mathbf{v}, \tag{5}$$

$$\frac{\partial \mathbf{b}}{\partial \tau}=\boldsymbol{\nabla}\times(\mathbf{v}\times\mathbf{b})+\frac{1}{S_\eta}\boldsymbol{\nabla}^2\mathbf{b}, \tag{6}$$

$$\frac{\partial T}{\partial \tau}+(\mathbf{v}\cdot\boldsymbol{\nabla})T+(\gamma-1)T(\boldsymbol{\nabla}\cdot\mathbf{v}) =\frac{\gamma-1}{\rho}\left[\frac{1}{S_\kappa}\boldsymbol{\nabla}^2T+\frac{1}{S_\nu}\left(\frac{\partial v_i}{\partial x_j}\frac{\partial v_i}{\partial x_j}\right)+\frac{1}{S_\eta}\mathbf{j}^2\right], \tag{7}$$

with $\mathbf{j}=\boldsymbol{\nabla}\times\mathbf{b}$ and $\gamma=5/3$ is the adiabatic index. The lengths are normalized to the shear length a, the magnetic field $\mathbf{b}$, and the mass density ρ, to the respective characteristic values B_0 and ρ_0, the velocities to the Alfvén velocity corresponding to these values. The time τ, pressure p, and temperature T, are normalized consistently. The quantities S_ν and S_η represent, respectively, the viscous and magnetic Reynolds numbers, while S_κ is a dimensionless number associated with the heat conductivity coefficient. Since dissipative coefficients are very low in solar wind we have used for the above quantities the largest values allowed by computer limitations: $S_\nu=S_\eta=S_\kappa/(\gamma-1)=1400$.

All quantities depend on two space variables (x and y), but vector quantities have three nonvanishing components. Equations (4)–(7) have been numerically solved in a rectangular spatial domain $D=[-l,l]\times[0,\pi Rl]$, with vanishing normal derivatives and periodic boundary conditions, along x and y, respectively.

The initial condition is given by a background nonuniform equilibrium, with a large amplitude fluctuation superimposed. The background equilibrium is a model for the large scale structure of a magnetic sector boundary; it contains two ingredients.

(a) A current sheet. The interplanetary magnetic field changes polarity going from one magnetic sector to another and a current sheet is associated to such a change. In our model we assume that the background magnetic field is parallel to the yz plane and depends only on x, which represents the direction of inhomogeneity. The y axis is the initial propagation direction of the perturbation. Increasing x, the background magnetic field accomplishes a rotation, the y component being positive (negative) for $x>0$ ($x<0$). This reproduces the change in polarity. A current sheet is associated to the magnetic field inhomogeneity: the current is directed along z and it is mainly concentrated in a layer of width $\simeq a=1$. The domain width ($2l=8$) is much larger than the current sheet.

(b) A large scale entropy modulation. The slow speed solar wind streams are colder and denser than the surrounding fast streams. In particular, the ion density and temperature are anticorrelated on a time scale ~ 1 day, the density displaying in many cases a rough maximum close to the current sheet location. In our model the background density and temperature vary along the cross-current-sheet (x) direction. The density is maximum and the temperature is minimum at the center $x=0$ of the current sheet, while the associated variation length $a_e=2$ is larger than the current sheet width a. The product ρT is initially uniform to ensure gas pressure equilibrium in the background structure. Correspondingly, the specific entropy s varies on the same scale a_e. As discussed in the Introduction, we expect that the nonlinear evolution of the perturbation induces an entropy cascade to smaller scales.

In order to single out the effects due to entropy modulation on the dynamical evolution, we neglect the velocity large scale variation associated to the stream structure. We assume a uniform background velocity, which is vanishing in a reference frame moving with the plasma. Solar wind observations [15] show that in many cases the magnetic sector boundary is totally embedded into slow-speed streams and that the typical length scale for the associated current sheet (some hours) is generally much less than the typical width of slow-speed streams (some days). In such cases neglecting background velocity inhomogeneities related to the stream structure is a reasonable approximation. We will discuss this point with reference to particular samples of the Helios data set, which will be examined in detail.

The large amplitude perturbation is Alfvénically correlated and it has opposite correlation on the two sides of the current sheet, so it propagates in the same direction. The magnitude $|\mathbf{B}|$ of the total magnetic field (background plus perturbation) is uniform. If the background medium were homogeneous, such a perturbation would propagate without distorsions. In Refs. [4] and [3] we have shown that both the presence of the current sheet and the interaction between the oppositely correlated Alfvénic fluctuations generate a dynamical evolution. The presence of the entropy modulation will further contribute to such an evolution. The largest wavelength $\lambda_{\max}$ of the perturbation in the periodicity direction is equal to the domain length. The value used for the aspect ratio $R=0.15$ corresponds to $\lambda_{\max}/a=3\pi/5$.

The initial condition is expressed by the following equations:

$$\rho(x,y,\tau=0)=\rho_0\left\{1+\Delta\left[\frac{1}{\cosh^2(x/a_e)}+p\left(\frac{x}{a_e}\right)^2\right]\right\}, \tag{8}$$

$$\mathbf{b}(x,y,\tau=0)=A\{\epsilon\cos[\phi(y)]\hat{\mathbf{e}}_x+\sin(\alpha)F(x)\hat{\mathbf{e}}_y +\sqrt{1-\sin^2(\alpha)F^2(x)+\epsilon^2\sin^2[\phi(y)]}\hat{\mathbf{e}}_z\}, \tag{9}$$

$$\mathbf{v}(x,y,\tau=0)=\sigma(x)\frac{\delta\mathbf{b}(x,y,\tau=0)}{\sqrt{\rho(x,y,\tau=0)}}, \tag{10}$$

$$T(x,y,\tau=0)=\rho_0T_0/\rho(x,y,\tau=0). \tag{11}$$

In the equation above

$$p=\frac{\tanh(l/a_e)}{(l/a_e)\cosh^2(x/a_e)}$$

is a parameter that ensures the fulfillment of the boundary conditions for the density and temperature, $\Delta=1/4$ is the amplitude of the entropy inhomogeneity, and the product ρ_0T_0 is the total, constant, kinetic pressure. The function $F(x)$ is defined by

$$F(x)=\frac{\tanh x - x/\cosh^2 l}{\tanh l - l/\cosh^2 l}. \tag{12}$$

The background magnetic field [obtained by putting $\epsilon=0$ in Eq. (9)] rotates by an angle 2α (we used $\alpha=\pi/4$ and $A=\sqrt{2}$). The parameter $\epsilon=0.5$ measures the amplitude of the Alfvénic perturbation and its spectrum is defined by $\phi(y)$, for which we used a power law

$$\phi(y)=2k_0\sum_{m=1}^{m_{\max}} m^{-5/3}(\cos mk_0), \tag{13}$$

where $k_0=2\pi/\lambda_{\max}$, and we have chosen $m_{\max}=32$. The fluctuating part δf of any quantity f is defined as

$$\delta f(x,y,\tau)=f(x,y,\tau)-\frac{1}{\pi R l}\int_0^{\pi R l} f(x,y,\tau)dy, \tag{14}$$

the solutions being periodic along the y direction.

We point out that in this initial condition, due to the density and temperature modulation [Eqs. (8) and (11)] both the Alfvén speed and the sound speed $c_s=[\gamma T_0(x,y,\tau=0)]^{1/2}$ (where γ is the adiabatic index) are not uniform, both becoming larger with increasing the distance from the current sheet. However, the plasma $\beta=c_s^2/c_A^2$ is still uniform in the entire domain.

III. COMPARISON BETWEEN NUMERICAL AND EXPERIMENTAL DATA

We are mainly interested in studying the compressive fluctuations produced by the interaction between Alfvénic fluctuations and the inhomogeneous background structure. In this analysis we studied the behavior of the correlation between compressive quantities: density, temperature, and magnetic field intensity. We define

$$\sigma_{fg}=\frac{\langle \Delta f \Delta g\rangle_{\Delta x}}{\sqrt{\langle(\Delta f)^2\rangle_{\Delta x}\langle(\Delta g)^2\rangle_{\Delta x}}}, \tag{15}$$

where $f=f(x,y)$ and $g=g(x,y)$ are two physical quantities and the angular brackets represent a running average over the length Δx:

$$\langle f\rangle_{\Delta x}=\frac{1}{\Delta x}\int_{-\Delta x/2}^{\Delta x/2} f(x+\xi,y,\tau)d\xi. \tag{16}$$

The quantities have been periodically extended for $|x|>l$ in order to compute the averages (16) in points closer to the boundaries $x=\pm l$ than $\Delta x/2$. The symbol Δf represents the difference $\Delta f=f-\langle f\rangle_{\Delta x}$, namely, the contribution to the field f owed to the scales smaller than Δx.

Plotting $\sigma_{fg}(x,y_0)$ as a function of x for a given value y_0 shows how the quantities f and g are correlated along a particular line $y=y_0$ crossing the current sheet. Such plots $\sigma_{fg}(x,y_0)$ generally keep the same qualitative behavior when changing the value of y_0, i.e., when moving along the direction of periodicity. Since we want to give a general information about the behavior of the correlation coefficient across the inhomogeneity, we will average it in the y direction, always considering the quantity $\langle\sigma_{fg}\rangle_y$. This also allows a more direct comparison between our results and the experimental data, where all the quantities are known along a one-dimensional trajectory.

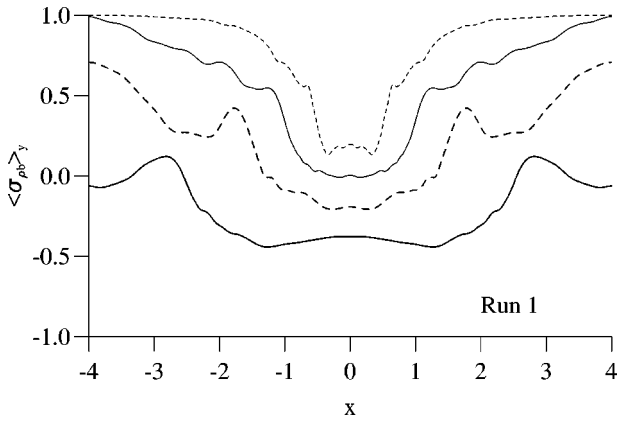

FIG. 1. Density–magnetic-field-intensity correlation $\langle\sigma_{\rho b}\rangle_y$ (averaged in the periodicity direction) at several length scales: $\Delta x=4.0$ (thick-solid line), $\Delta x=2.0$ (thick-dashed line), $\Delta x=1.0$ (thin-solid line), and $\Delta x=0.5$ (thin-dashed line) for run 1 ($\beta=0.2$). The time is $\tau=4.8$ (dimensionless units).

As in paper I, we carried out three runs, named runs 1, 2, and 3, with different values of the plasma β parameter:

$$\beta=\frac{c_s^2}{c_A^2}=\frac{4\pi\gamma k_B\rho T}{B_0^2}, \tag{17}$$

where k_B is the Boltzmann's constant. We used the values $\beta=0.2$, 1.0, 1.5, respectively, as in paper I, in order to compare the numerical results with the observations.

A. Density–Magnetic-field-intensity correlation

We have performed a study of the density–magnetic-field-intensity correlations as we did in paper I. The initial condition is different from the one used in paper I, in that both density and temperature in the background structure are spatially modulated. This further inhomogeneity contributes to the dynamical evolution of the initial Alfvénic perturbation, and the resulting ρ-b correlation could in principle be different from that found in paper I. For this reason, it is useful to compare the ρ-b correlation as it results in the two models.

In Fig. 1, the correlation coefficient $\langle\sigma_{\rho b}\rangle_y$, averaged in the y direction, is plotted. This graph is relative to run 1 (low β) and the values used for the length scale Δx are $\Delta x=0.5$, 1.0, 2.0, and 4.0. These values are the same used in paper I, as well as the time in which the correlation is calculated. Comparing the plots in Fig. 1 with those in Fig. 1 of paper I, it can be seen that in both cases the ρ-b correlation tends to be more negative close to the current sheet than in the homogeneous region. However, this tendency is stronger in the model of paper I, in particular at smaller scales ($\Delta x\leqslant 2$): in the present model the correlation is close to zero in the current sheet and positive in the homogeneous region, while in the model of paper I it is negative in the current sheet and with an undefined sign in the homogeneous region. Thus, the presence of the large scale entropy modulation

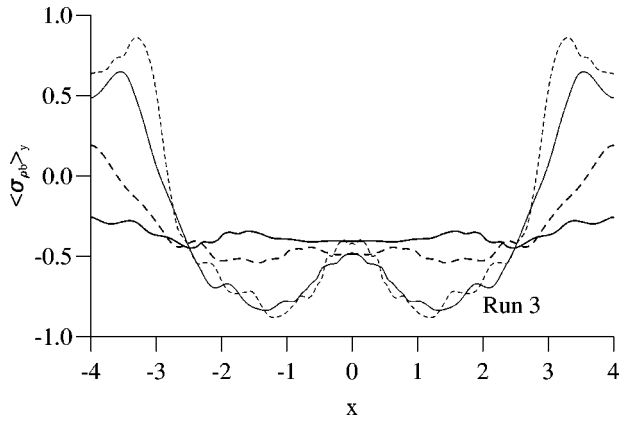

FIG. 2. Same plot as in Fig. 1 but for run 3 ($\beta=1.5$) at time $\tau=4.2$.

seems to reduce the generation of small scale slow magnetosoniclike fluctuations, with a comparatively larger abundance of positive correlated fluctuations, at least for small values of β.

In Fig. 2 the correlation coefficient $\langle\sigma_{\rho b}\rangle_y$ is plotted, relative to run 2, in which $\beta=1$. Comparing these results with those shown in Fig. 2 of paper I, it is seen that the behavior of the ρ-b correlation in the two models is now very similar. In both cases the negative correlation prevails in a wide region around the current sheet, while it is mainly positive close to the boundaries. In a similar way, the results of run 3 at $\beta=1.5$ (not shown) are very close to the corresponding results obtained from the model of paper I (Fig. 3 of paper I). Then, for β of the order or larger than 1 the presence of the entropy modulation in the background structure does not modify the behavior of the ρ-b correlation, at the considered scales.

The results of the model of paper I had been compared with the density–magnetic-field-intensity correlation calculated during periods of the Helios data set, finding good agreement. In all those periods $\beta\geqslant 1$. Then, we can conclude that the same good agreement exists also between the ρ-b correlation calculated in the present model and the corresponding quantity observed in the considered Helios data.

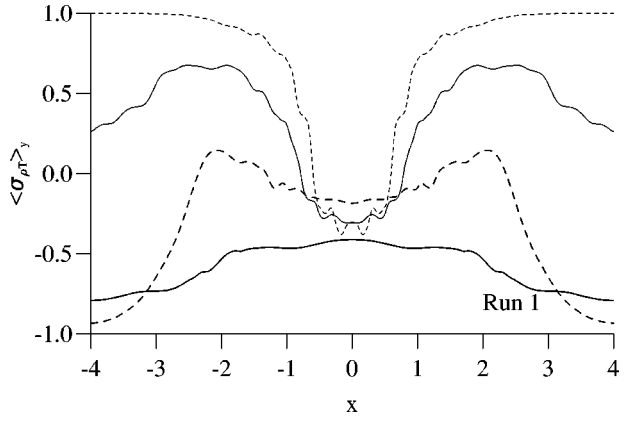

FIG. 3. Density-temperature correlation $\langle\sigma_{\rho T}\rangle_y$ (averaged in the periodicity direction) at several length scales: $\Delta x=4.0$ (thick-solid line), $\Delta x=2.0$ (thick-dashed line), $\Delta x=1.0$ (thin-solid line), and $\Delta x=0.5$ (thin-dashed line) for run 1 ($\beta=0.2$). The time is $\tau=4.8$ (dimensionless units).

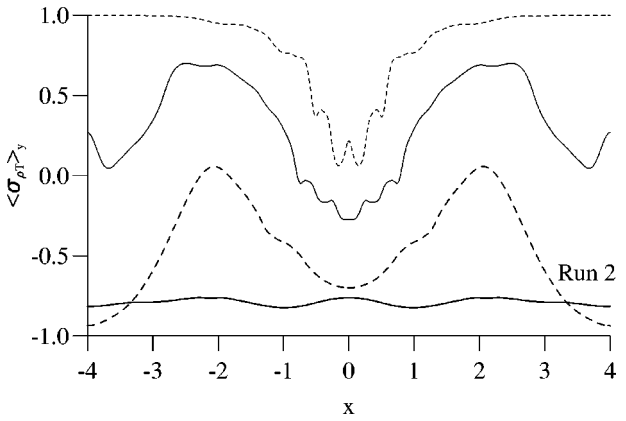

FIG. 4. Same plot as in Fig. 3 but for run 2 ($\beta=1.0$) at time $\tau=4.2$

B. Density-temperature correlations

In Fig. 3 we show the plots of the quantity $\langle\sigma_{\rho T}\rangle_y$ at different length scales $\Delta x=0.5$, 1.0, 2.0, and 4.0 for run 1. We remember that the length unit corresponds to the half width of the current sheet. The quantities are plotted at a time $\tau=4.8$. This time corresponds to few eddy turnover times, so nonlinear effects have had enough time to build up the spectrum [3]. One can see that, when averaging on the whole domain, a negative density-temperature correlation prevails at large scale, while $\langle\sigma_{\rho T}\rangle_y$ tends to become increasingly positive with decreasing the scale Δx.

The detailed behavior of $\langle\sigma_{\rho T}\rangle_y$ is different at different scales Δx: at large scale the correlation is negative in the whole domain; decreasing the scale $\langle\sigma_{\rho T}\rangle_y$ remains slightly negative at the center of the domain, while it becomes more and more positive close to the boundaries, i.e., far from the inhomogeneity region.

The negative correlation at larger scales essentially reflects the entropy modulation of the background structure, which was present in the initial condition. The behavior of $\langle\sigma_{\rho T}\rangle_y$ at smaller scales indicates that in the region where the background structure is more inhomogeneous small scale entropy fluctuations prevail; such fluctuations should result from an entropy cascade from large to small scales. In the region where the background structure is more homogeneous, magnetosoniclike fluctuations dominate. In this same region, the density–magnetic-field-intensity correlation is positive too (see Fig. 1). This indicates that small scale compressive fluctuations in the homogeneous region essentially have properties similar to those of the fast magnetosonic mode.

In Fig. 4, the same plot as in Fig. 3 is shown for a higher value $\beta=1.0$ (run 2), at a different time $\tau=4.2$. We chose an earlier time because for higher βs the compressive phenomena have shorter characteristic time scales. One can notice that the behavior is similar to the previous case, even though there is a stronger tendency to generate positive ρ-T correlations at small scales with respect to the lower β run. In particular, on larger scales the anticorrelations are dominant everywhere in the simulation domain. On smaller scales the sign of the correlation is positive close to the boundaries, while in the central region $\langle\sigma_{\rho T}\rangle_y$ is slightly negative or very close to zero, according to the value of Δx. A further run (run 3) was carried out with a bigger value $\beta=1.5$; the cor-

TABLE I. Quantities relative to the data in Figs. 5–8.

Parameters	$H1$	$H2$	$H3$	$H4$
$t_{start}-t_{end}$ (days)	45.9–46.9	54.5–55.5	80.7–81.7	19.5–20.5
R (AU)	0.905	0.85	0.6	0.98
$\langle\beta\rangle$	$\sim$1.0	$\sim$5.1	$\sim$2.9	$\sim$1.5

responding plots are very similar to those obtained in the case $\beta=1.0$.

We point out that the plots of Figs. 3 and 4 illustrate the situation averaged along the periodicity direction. A look at the two-dimensional contour plots of $\sigma_{\rho T}$ (not showed here) demonstrates that small scale fluctuations both with a clear negative correlation and with a positive correlation are present in the central inhomogeneity region, with a slight prevalence of the former over the latter. Such fluctuations appear to be localized in different positions along y. Thus, particular ''cuts'' $\sigma_{\rho T}(x,y_0)$ would show positive or negative small scale correlation in the central region, according to the particular position y_0. In this sense the plots of Figs. 3,4 can be considered as representative of the (statistical) mean behavior of the density-temperature correlation, averaged over several crossings of slow speed streams. Then, the results of Figs. 3 and 4 cannot reproduce the detailed behavior of the correlation during a particular data period. Rather, they should be compared with general features displayed by the density-temperature correlation in several slow speed stream crossings.

Let us now consider the analogous analysis for the observations. For this we used data from the Helios 2 mission. We studied the correlation between proton density n and temperature T_p, assuming the behavior of the proton temperature in slow speed streams as representative of that of the total temperature T_p+T_e [6]. The correlation σ_{nT} has been calculated for several periods, each containing a sector boundary. We selected, in particular, four periods (denoted by $H1,\ldots,H4$) in which the large scale structure is more similar to the one used in our model: namely, the maximum of proton density is near to the location of the heliospheric current sheet. These periods are listed in Table I, along with the distance R from the Sun and the value of the plasma β.

In Fig. 5 hourly averages (top panel) of the proton density and temperature are shown for the selected $H1$ period, along with the correlation coefficient σ_{nT} (bottom panel) calculated on various time scales $\Delta t=2$, 6, 12, 24 h. Assuming a shear crossing time $t_a\sim 6$ h, those times roughly correspond to the scale lengths Δx used in the simulations. The data have been hourly averaged before working out the correlations, in order to filter out the oscillations uninteresting for our comparison and that degenerate the clearness of the plots. For this period, it is $\beta\sim 1$. The magnetic field changes sign in proximity of $t\sim 46.4$ (as shown by Pilipp *et al.* [15]), while the position of the heliospheric current sheet is denoted by a thick segment on horizontal axis (top panel). At that location the density has a bump and the temperature a hole. These conditions correspond to those we used in our simulations. It is apparent from the plot that, corresponding to the density peak, σ_{nT} has a negative sign at all time scales. Far from both the current sheet and the density maximum the sign of correlation becomes increasingly positive by going towards smaller scales. The qualitative behavior is in fairly good agreement with the trend observed in the simulations.

A similar situation is represented in Fig. 6, where the same plot as in Fig. 5 is shown for the period $H2$. In this case, the value of β is much higher $\beta\sim 5.1$. The position of density peak appears slightly displaced with respect to the current sheet. The behavior of the correlation is akin to that observed at smaller β (Fig. 5). Again, in correspondence of the density peak σ_{nT} is negative at all time scales. Moving away from the density peak, σ_{nT} is still negative at large scales, becoming positive at small scales.

Another case with high β is shown in Fig. 7, that corresponds to the period $H3$ in Table I. Also in this case, the trend is similar to the one observed in the previous periods. A well defined density peak (corresponding to the zone where the magnetic field changes polarity) is embedded between two temperature bumps. Again the correlation is nega-

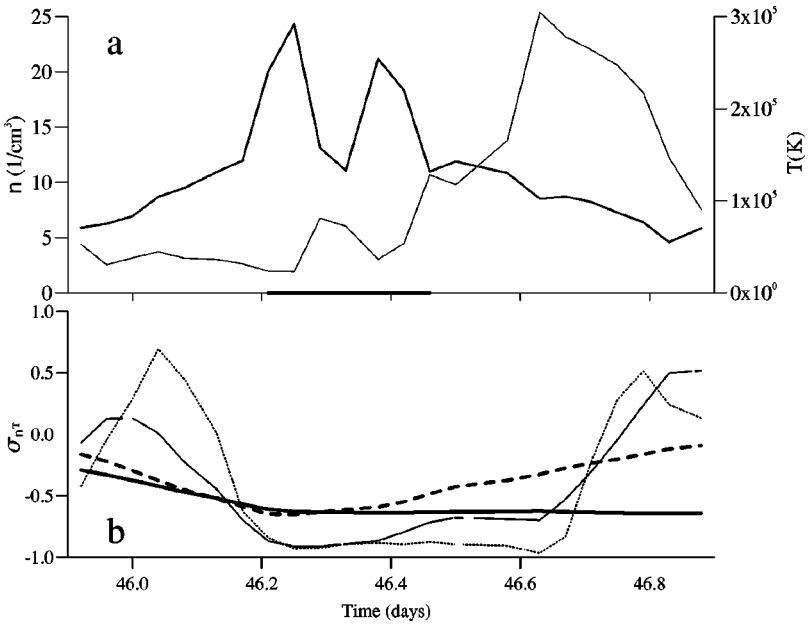

FIG. 5. (a) Hourly averages of the density (thick line) and temperature (thin line) for the period $H1$. (b) Values of the density-temperature correlation σ_{nT} at different time scales: $\Delta t=24$ h (thick-solid line), 12 h (thick-dashed line), 6 h (thin-solid line), and 2 h (thin-dashed line) for the same period (data from the Helios 2 data set of year 1976).

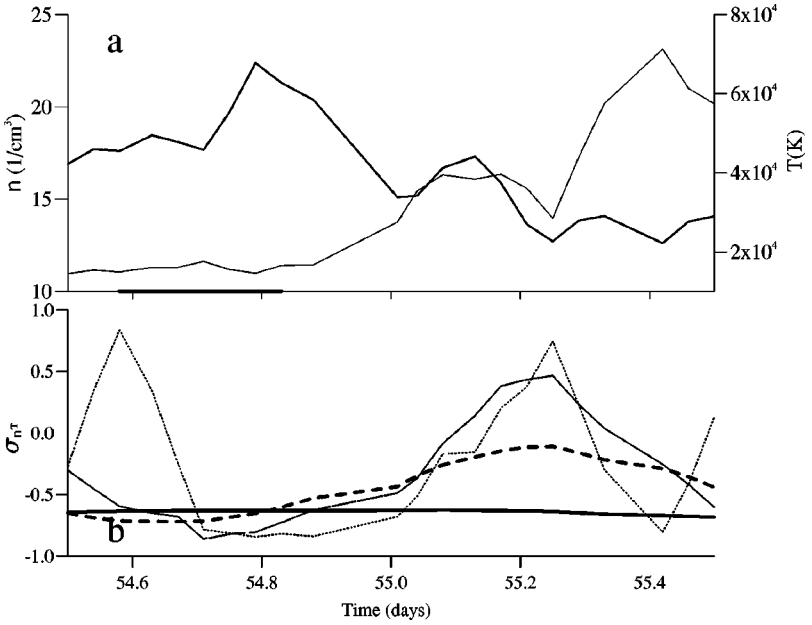

FIG. 6. Quantities in the same format as in Fig. 5 but for period $H2$.

tive at all scales where the density is higher, and positive at small scales on the wings. The last case, shown in Fig. 8, is relative to the period $H4$, in which $\beta \sim 1.5$. Also in this case, the behavior of density-temperature correlation is similar to that described above.

In summary, the behavior displayed by σ_{nT} as a function of both position (close or far from the current sheet and density maximum) and time scale, in the considered periods of the Helios data set, is essentially reproduced by our model. Moreover, the above described features of σ_{nT} appear to be essentially independent of the value of β; this is also verified for the ρ-T correlation, as it results from our model.

IV. DISCUSSION AND CONCLUSIONS

In this paper we have built up a model to describe the generation of both positive and negative correlations between density and temperature fluctuations in solar wind slow speed streams. In a previous model (Ref. [3], paper I) interactions among two fluxes of oppositely correlated Alfvénic fluctuations and a large scale current sheet have been studied, in order to describe the formation of compressive fluctuations around the heliospheric current sheet. This model predicts that the correlation between density and magnetic field intensity changes according to length scale, location (close or far from the current sheet) and value of β. Such results compare well with the behavior of the proton density–magnetic-field-intensity correlation in slow speed streams, as calculated from space data (paper I). In the model of paper I, density, temperature, and entropy per-mass-unit s are initially uniform. Then, from Eq. (1) it follows that s keeps uniform also at subsequent times, except for the effects of dissipation and/or thermal conduction. Such effects can modulate s, but essentially at small scales. In consequence of this quasi-isoentropic state, fluctuations of ρ and T have been found to be always positively correlated [Eq. (3)]. In other

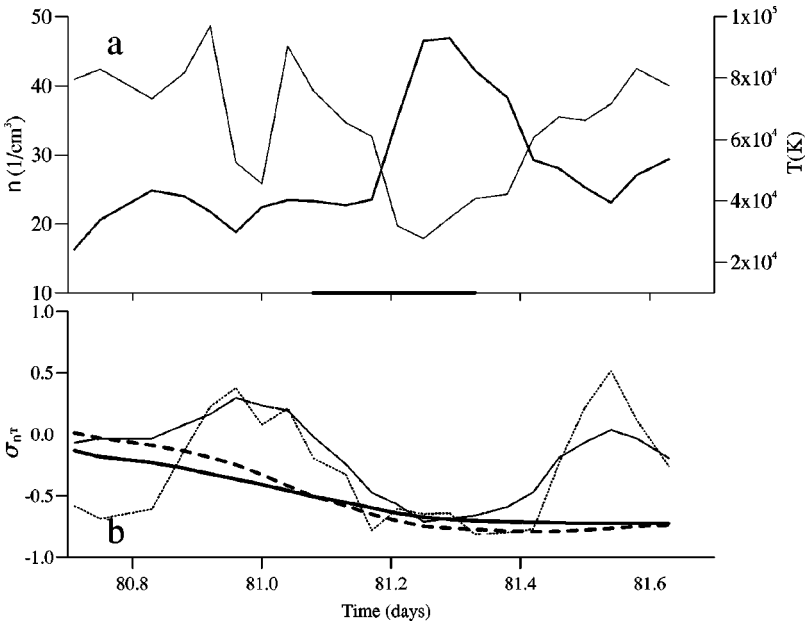

FIG. 7. Quantities in the same format as in Fig. 5 but for period $H3$.

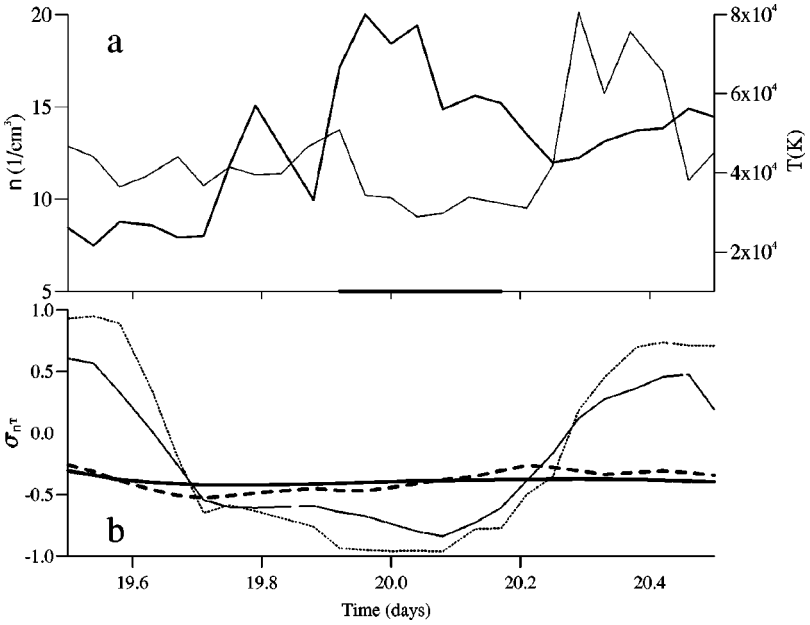

FIG. 8. Quantities in the same format as in Fig. 5 but for period $H4$.

words, compressive fluctuations generated in the model of paper I are only of magnetosonic nature (fast and slow). This is in contrast with observations, since both positive and negative n-T_p correlation has been found in solar wind data [8].

The present model represents an improvement of the previous one, in that both positive and negative ρ-T correlation is produced. The model includes, as a new ingredient, a large scale variation of both density and temperature: when moving away from the current sheet, ρ decreases and T increases, corresponding to a large scale variation of the entropy per-mass-unit s. The observed proton density is typically higher and temperature is lower in a slow speed stream than in the surrounding high speed streams. In many cases gas pressure equilibrium postulated in our model does not hold in solar wind. However, at large scales n and T_p are always anticorrelated (see Figs. 5–8); this implies a large scale modulation of the entropy, which represents the main physical ingredient of our model. Neglecting the small nonideal terms, Eq. (1) indicates that s is convected by fluid motion as a passive scalar: the turbulent velocity field (essentially generated close to the current sheet [3]) extends the modulation of s to increasingly small scales. Such an entropy cascade accounts for the production of ρ-T anticorrelations at all the scales. This mechanism acts in competition with the generation of magnetosoniclike fluctuations [3], in which the ρ-T correlation is positive.

Concerning this point, we note that, while negative ρ-T correlations necessarily requires an entropy modulation, in a nonisoentropic state positive and negative ρ-T correlations coexist. In other words, a situation can be figured, in which magnetosoniclike fluctuations and entropy modulations are superposed. This kind of situation has been considered by Malara *et al.* [16] who studied the formation of small scales in a small amplitude disturbance, propagating in a nonuniform plasma. Decomposing the perturbation as a superposition of linear modes, it was shown that both magnetosonic waves and static entropy waves had been generated, the former with a positive and the latter with a negative ρ-T correlation [16].

In the large amplitude, nonlinear situation considered in the present paper it is not possible to separate the solution as a superposition of modes. However, both signs of the ρ-T correlation can be found; in case of positive correlation we can think that fluctuations of magnetosonic origin dominate at the given location and/or spatial scale, while in case of negative correlation the modulation of the entropy prevails.

The results obtained by our model have been compared with the proton density-temperature correlation σ_{nT} in solar wind slow speed streams, considering several samples of the Helios spacecraft data set. We have found that the dependence of σ_{nT} both on location (close or far from the current sheet) and on the fluctuation scale is qualitatively reproduced by the numerical model. Moreover, the behavior of this correlation does not show a significant dependence on the value of β, both in the simulation results and in data analysis. These similarities indicate that the main physical mechanisms which determine the density-temperature correlation observed in slow speed streams have been included in our model. So, we can try to give a physical interpretation for the n-T_p correlation observed in the vicinity of the heliospheric current sheet.

The results of our model show that the anticorrelation between ρ and T, initially present only at large scales, is gradually extended toward small scales. This process is effective mainly in the inhomogeneous region, where negative correlation forms at all the considered spatial scales. As shown in Malara *et al.* [3], in the current sheet region a strong turbulence forms, due both to the interaction between oppositely correlated Alfvénic fluctuations and to the large scale inhomogeneity. This inhomogeneity has now become more complex because of the presence of the large scale modulation of density and temperature. As discussed above, the turbulence which develops in the inhomogeneous region acts on the entropy modulation present in the background configuration, by ''mixing'' the spatial structure of s and generating an entropy cascade.

On the other hand, in Malara *et al.* [3] it has been shown that the turbulence close to the current sheet contains compressive slow magnetosoniclike fluctuations, at all the con-

sidered scales. This same phenomenon happens also when a large scale density and temperature modulation is included, since the behavior of the ρ-B correlation is similar to that found in the previous model. Then, the prevalence of negative n-T_p correlation at small scales in solar wind data, indicates that, close to the current sheet the entropy cascade is dominant with respect to the generation of magnetosonic fluctuations.

Far from the current sheet, our results indicate that the ρ-T correlation is negative at large scales, but it becomes increasingly positive when decreasing the spatial scale. This fact can be understood thinking that in this region variations in density and temperature of the background structure are reduced with respect to the central region. So, the equilibrium is closer to an isoentropic condition. Correspondingly, the efficiency of the entropy cascade is reduced. At the same time, far from the current sheet, other mechanisms, such as parametric decay, are at work to generate a spectrum of compressive fluctuations, which extends to small scales (Malara *et al.* [3]). Such fluctuations belong to the magnetosonic mode, so the associated density and temperature fluctuations are positively correlated. The positive n-T_p correlation found in such region at small scales indicates that the latter mechanisms dominate on the entropy cascade. On the contrary, the negative correlation at large scales implies that no relevant magnetosonic fluctuations are produced at large scales, so that the negative n-T_p correlation of the background structure remains essentially unaffected by the dynamical evolution.

Bavassano *et al.* [8] studied the proton density-temperature correlation for fluctuations at frequencies of 45 min and 3 h, that are both in our ''small-scale'' range. They found that, while in fast speed streams such correlation is essentially positive, cases with both signs are found in slow speed streams. This fact again supports the idea that negative correlations found in slow speed streams can be understood in terms of a large scale entropy modulation and a subsequent entropy cascade generated by the dynamical evolution. These phenomena are not relevant in fast streams, the background large scale structure being more homogeneous than in slow streams.

Let us discuss briefly the validity of our assumptions, in particular the fact that we neglected the velocity field shear in our simulations. For each one of the periods in Table I we plotted separately (these plots are not shown here) the proton velocity as a function of time. In all the cases except period $H1$, we found that the average speed never exceeded 400 Km/s and its profile was roughly flat. This means the selected intervals were always embedded in remarkably uniform slow speed streams. Moreover, for periods $H2$ and $H3$ the velocity shows only very slow variations during four days, before and after the current sheet, while the transition between slow and fast wind is located well outside period $H4$. A more important velocity variation is present during period $H1$, in which the velocity increases of about 160 Km/s in 20 h, but this variation is clearly smaller than those associated to the stream structure. In summary, our model in which the stream structure has been neglected applies well to periods $H2$, $H3$, and $H4$, while it represents a reasonable approximation for period $H1$, and we can assume that in these periods the considered correlations should not be influenced by the stream structure.

The results of this model and comparisons with solar wind data indicate that the large scale inhomogeneity associated to slow speed streams and to the heliospheric current sheet plays an important role in determining major features of compressive fluctuations. In particular, the observed density-temperature correlation can be due to the presence of an entropy cascade and to the generation of a spectrum of magnetosonic fluctuations. Both phenomena are driven by the dynamical interaction between Alfvén waves propagating away from the Sun and nonuniformities intrinsic to the large scale configuration of the background medium. Then, models treating the MHD turbulence in slow speed streams should include inhomogeneity effects.

ACKNOWLEDGMENTS

This work is part of a research program that is financially supported by the Ministero dell'Università e della Ricerca Scientifica e Tecnologica (MURST), the Consiglio Nazionale delle Ricerche (CNR), under Contract No. 98.00148.CT02, and the Agenzia Spaziale Italiana (ASI) under Contract No. ARS 98-82.

[1] M. Vellante and A. J. Lazarus, J. Geophys. Res. **92**, 9893 (1987).
[2] E. Marsch and C. Y. Tu, Ann. Geophys. (C.N.R.S.) **11**, 659 (1993).
[3] F. Malara, L. Primavera, and P. Veltri, J. Geophys. Res. **101**, 21 597 (1996).
[4] F. Malara, P. Veltri, and L. Primavera, Phys. Rev. E **56**, 3508 (1997).
[5] L. Klein, R. Bruno, B. Bavassano, and H. Rosenbauer, J. Geophys. Res. **98**, 7837 (1993).
[6] E. Marsch and C. Y. Tu, Ann. Geophys. (C.N.R.S.) **11**, 659 (1993).
[7] C. Y. Tu and E. Marsch, J. Geophys. Res. **99**, 21 481 (1994).
[8] B. Bavassano, R. Bruno, and L. W. Klein, J. Geophys. Res. **100**, 5871 (1995).
[9] W. H. Matthaeus and M. R. Brown, Phys. Fluids **31**, 3634 (1988).
[10] G. P. Zank and W. H. Matthaeus, Phys. Rev. Lett. **64**, 1243 (1990).
[11] W. H. Matthaeus, L. W. Klein, S. Ghosh, and M. R. Brown, J. Geophys. Res. **96**, 5421 (1991).
[12] G. P. Zank and W. H. Matthaeus, Phys. Fluids A **3**, 69 (1991).
[13] G. P. Zank and W. H. Matthaeus, Phys. Fluids A **5**,257 (1993).
[14] A. I. Akhiezer, I. A. Akhiezer, R. V. Polovin, A. G. Sitenko, and K. N. Stepanov, *Plasma Electrodynamics* (Pergamon, New York, 1975), Vol. 1.
[15] W. G. Pilipp, H. Miggenrieder, K.-H. Mühlhäuser, H. Rosenbauer, and R. Schwenn, J. Geophys. Res. **95**, 6305 (1990).
[16] F. Malara, L. Primavera, and P. Veltri, Astrophys. J. **459**, 347 (1996).